Speeding Up Future Video Distribution via Channel-Aware Caching-Aided Coded Multicast

Angela Sara Cacciapuoti, *Senior Member, IEEE*, Marcello Caleffi, *Senior Member, IEEE*, Mingyue Ji, *Member, IEEE*, Jaime Llorca, *Member, IEEE*, and Antonia Maria Tulino, *Fellow, IEEE*

***Abstract*— Future Internet usage will be dominated by the consumption of a rich variety of online multimedia services accessed from an exponentially growing number of multimedia capable mobile devices. As such, future Internet designs will be challenged to provide solutions that can deliver bandwidth-intensive delay-sensitive on-demand video-based services over increasingly crowded and bandwidth-limited wireless access networks. One of the main reasons for the bandwidth stress facing wireless network operators is the difficulty to exploit the multicast nature of the wireless medium when wireless users or access points rarely experience the same channel conditions or access the same content at the same time. In this paper, we present and analyze a novel wireless video delivery paradigm based on the combined use of channel-aware caching and coded multicasting that allows simultaneously serving multiple cache-enabled receivers that may be requesting different content and experiencing different channel conditions. To this end, we reformulate the caching-aided coded multicast problem as a joint source-channel coding problem and design an achievable scheme that preserves the cache-enabled multiplicative throughput gains of the error-free scenario, by guaranteeing per-receiver rates unaffected by the presence of receivers with worse channel conditions.**

***Index Terms*— Video distribution, coded multicast, caching, wireless channel, degraded broadcast channel.**

I. Introduction

THE latest projections [1], [2] suggest that, by 2019, mobile data traffic will increase nearly tenfold with respect to 2014, accounting for nearly two-thirds of the total data traffic. Furthermore, it is predicted that nearly three-fourths of the mobile data traffic will be video by 2019. In line with these trends, this paper considers the design and analysis of a novel wireless video delivery paradigm that specifically addresses two of the major predicted shifts of the Future Internet, i.e., *from fixed to mobile* and *from cable video consumption to IP video consumption*, by pushing caching to the wireless edge and exploiting the multicast nature of the wireless medium via channel-aware coded multicasting.

Recent works have addressed the design of heterogeneous wireless access networks composed of a combination of macro-, micro-, and pico-cells integrated within the cellular infrastructure, with the main advantage of the increased spatial reuse resulting from the simultaneous localized high-bandwidth wireless connections from small cell base stations to user devices. However, in many cases, the high cost incurred in wiring the small cells results in a shift of the bandwidth bottleneck to the wireless backhaul that serves the multiple access points. To alleviate this problem, recent works have proposed the use of a caching directly at the wireless edge, e.g., at wireless access points or end user devices, with the goal of reducing both latency and wireless backhaul requirements when serving video content (see [3] and references therein). In this context, recent information theoretic studies have shown that the use of network coding over the wireless backhaul can significantly improve the performance of wireless caching networks by creating cache-enabled coded multicast transmissions useful for multiple users (access points) even if requesting different content. In fact, is has been shown that the use of wireless edge caching and coded multicasting enables multiplicative caching gains, in the sense that the per-user throughput scales linearly with the local cache size [4]–[11]. However, the underlying assumption in existing information theoretic literature on caching networks is that the channels between the content source and the users either exhibit the same qualities or follow a shared error-free deterministic model. In practice, wireless channels are affected by impairments, such as multipath and shadow fading, and they must be modeled as non-deterministic noisy channels. Furthermore, different wireless channels can exhibit significant differences in their qualities, i.e., admissible throughputs, even when the users are closely located. This channel heterogeneity can significantly degrade the performance of any multicast-based approach in which the worst-channel user dictates the overall system performance [12], [13].

In the following, we address these open problems by considering a heterogeneous wireless edge caching architecture, as shown in Figure 1. It is composed of a macro-cell

Manuscript received May 29, 2015; revised December 6, 2015; accepted February 16, 2016. Date of publication June 6, 2016; date of current version August 11, 2016. This work was supported in part by the PON Projects FERSAT: Studio di un sistema di segnalamento FERroviario basato sull'innovativo utilizzo delle tecnologie SATellitari e della loro integrazione con le tecnologie terrestri and DATABANC CHIS: Cultural Heritage Information System, and in part by the Campania POR Project myOpenGov.

A. S. Cacciapuoti and M. Caleffi are with the Department of Electrical Engineering and Information Technology, University of Naples Federico II, Naples 80125, Italy (e-mail: angelasara.cacciapuoti@unina.it; marcello.caleffi@unina.it).

M. Ji is with Broadcom Ltd., San Jose, CA 92127 USA, and also with the University of Southern California, Los Angeles, CA 90089 USA (e-mail: mingyue.ji@broadcom.com).

J. Llorca is with Nokia Bell Labs, Murray Hill, NJ 07974 USA (e-mail: jaime.llorca@nokia.com).

A. M. Tulino is with the Department of Electrical Engineering and Information Technology, University of Naples Federico II, Naples 80125, Italy, and also with Nokia Bell Labs, Murray Hill, NJ 07974 USA (e-mail: antoniamaria.tulino@unina.it).

Color versions of one or more of the figures in this paper are available online at http://ieeexplore.ieee.org.

Digital Object Identifier 10.1109/JSAC.2016.2577198

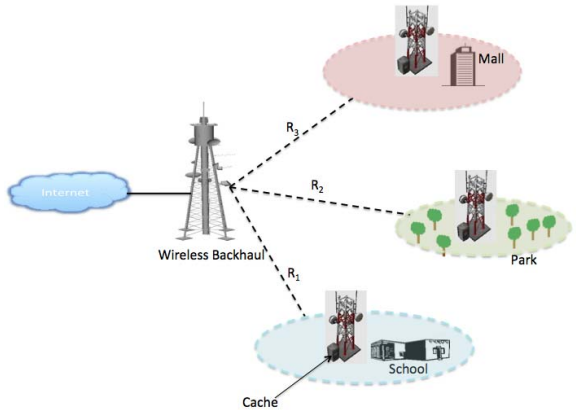

Fig. 1. Network model.

base station (BS) that distributes video content to a number of mobile devices, with the help of dedicated cache-enabled small cell base stations or wireless access points, referred to as *helpers*. Specifically, by exploiting the helper caching capabilities, the BS distributes the video content through coded multicast transmissions, reducing both content distribution latencies as well as overall network load [3], [8]. We model the channel between macro BS and helpers as a stochastically degraded broadcast channel. Our approach is based on formulating the caching-aided coded multicast problem over a noisy broadcast channel as a *joint source-channel coding problem*, in order to optimize the sharing of bandwidth and caching resources among cache-enabled receivers downstream of a common broadcast link with heterogeneous channel conditions. Our contributions can be summarized as follows:

- An information theoretic framework for wireless video distribution that takes into account the specific characteristics of the wireless propagation channel in the presence of any combination of unicast/multicast transmission and wireless edge caching;
- A channel-aware caching-aided coded multicast video delivery scheme, referred to as Random Popularity based caching and Channel-Aware Chromatic-number Index Coding (RAP-CA-CIC), that guarantees a rate to each receiver within a constant factor of the optimal rate had the remaining users experienced its same channel conditions, i.e., completely avoiding throughput penalizations from the presence of receivers with worse propagation conditions.
- A polynomial-time approximation of RAP-CA-CIC, referred to as Random Popularity based caching and Channel-Aware Hierarchical greedy Coloring (RAP-CA-HgC) with running time at most cubic in the number of receivers and quadratic in the number of (per-receiver) requested video descriptions.

The rest of the paper is organized as follows. Section II describes the network and video distribution models. Section III presents an information-theoretic formulation for the caching-aided wireless video delivery problem over a degraded broadcast channel. In Sections IV and V, we specialize the aforementioned information-theoretic formulation for a specific choice of the cache encoder (Sec. IV) and of the joint source-channel multicast encoder (Sec. V), introducing the proposed RAP-CA-CIC and RAP-CA-HgC algorithms. Detailed descriptions of CA-CIC and its polynomial-time approximation CA-HgC are given in Section VI. In Section VII, we describe the multicast decoder and the overall achievable performance. Section VIII presents simulation results for the proposed and state of the art schemes, along with related discussions. We conclude the paper in Section IX.

II. System Model

A. Network Model

We consider a wireless broadcast caching network consisting of a sender node (base station) and U receiver nodes (helpers) $\mathcal{U} = \{1, \dots, U\}$, as shown in Figure 1. The sender has access to a content library $\mathcal{F} = \{1, \dots, m\}$ containing m files, where each file has entropy F bits. Each receiver $u \in \mathcal{U}$ has a cache with storage capacity $M_u F$ bits (i.e., M_u files). We denote by $M_{u,f}$ the fraction of file $f \in \mathcal{F}$ stored at receiver u, such that $\sum_f M_{u,f} \leq M_u$. Without loss of generality, the files are represented by binary vectors $W_f \in \mathbb{F}_2^F$.

Differently from existing works for this network [4]–[10], here the sender is connected to the receivers via lossy links. Specifically, we model the links between the sender and the receivers as stochastically degraded binary broadcast channel (BC). The processes governing the links time evolution are assumed to be stationary and ergodic. While the binary field is specially convenient for ease of presentation, our approach can be extended to general stochastically degraded broadcast channels [14], with the case of arbitrary additive noise broadcast channels being particularly immediate. Our analysis includes both a binary symmetric broadcast channel (BS-BC) and a binary erasure broadcast channel (BE-BC).

- **BS-BC Case**: The channel output $Y_u[t]$ observed by the u-th receiver at the t-th channel use takes values in the binary alphabet $\mathcal{Y} \equiv \{0, 1\}$ and is given by

$$Y_u[t] = X[t] + Z_u[t], \tag{1}$$

  where $X[t]$ denotes the binary encoded symbol sent by the sender at the t-th channel use, and $Z_u[t]$ denotes the additive noise of the channel corresponding to receiver u, modeled as a Bernoullian variable with parameter given by the channel degradation ϵ_u, i.e., $Z[t] \sim \mathcal{B}(\epsilon_u)$. Letting η_u denote the achievable channel rate, we have

$$\eta_u \leq 1 - H(\epsilon_u), \tag{2}$$

  with $H(\epsilon_u)$ denoting the binary entropy function.
- **BE-BC Case**: The channel output $Y_u[t]$ observed by the u-th receiver at the t-th channel use exactly reproduces the channel input $X[t]$ with probability $(1 - \epsilon_u)$ and otherwise indicates an erasure event, with probability ϵ_u. In this case, $Y_u[t]$ takes values in the ternary alphabet $\mathcal{Y} \equiv \{0, 1, \star\}$ so that an erasure event is represented by the erasure symbol "$\star$". The achievable channel rate η_u then satisfies

$$\eta_u \leq 1 - \epsilon_u. \tag{3}$$

B. Video Distribution Model

We consider a video streaming application, in which each file $f \in \mathcal{F}$ represents a video segment, which is multiple description coded[1] into D descriptions using, for example, one of the coding schemes described in [12] and [16]. Each description is packaged into one information unit or packet for transmission. Each packet is represented by a binary vector of length (entropy) $B = F/D$ bits. A low-quality version of the content can be reconstructed once a receiver is able to recover any description. The reconstruction quality improves by recovering additional descriptions and depends solely on the number of descriptions recovered, irrespective of the particular recovered collection. Hence, there are D video qualities per segment, where the entropy in bits of quality $d \in \{1, \ldots, D\}$, containing d descriptions, is given by $F_d = Bd$. Note that in video streaming applications, every video segment has the same (playback) duration, which we denote by Δ in time units (or channel uses). Hence, the difference in quality levels solely depends on the number of bits F_d. In practice, the video segment duration should be chosen according to the maximum quality offered by the video application and the channel conditions [17]. In this paper, we set $\Delta = \gamma F$, with $\gamma > 0$ being a system parameter that depends on the channel conditions.

Video segments are characterized by a popularity or *demand distribution* $\mathbf{Q} = [q_{f,u}], u = 1, \cdots, U, f = 1, \cdots, m$, where $q_{f,u} \in [0, 1]$ and $\sum_{f=1}^{m} q_{f,u} = 1$ (e.g., receiver u requests file f with probability $q_{f,u}$). Let f_u denote the random request at receiver u. The realization of f_u is denoted by f_u.

It is important to note that this paper considers a general video on-demand setting, in which receiver requests follow an arbitrary popularity distribution. As such, the demand message set cannot be represented as a *degraded message set* [18], [19] since a given receiver's demand is not necessarily a subset of another receiver's demand. Our demand model includes and generalizes any combination of degraded message sets, via possible overlapping of receiver demands, and message cognition, via available cached or side information [20].

We consider a video delivery system that operates in two phases: a caching phase[2] followed by a transmission phase.

- **Caching Phase:** The caching phase occurs during a period of low network traffic. In this phase, using the knowledge of the demand distribution and the cache capacity constraints, the sender decides what content to store at each receiver. We denote by $\mu_{u,f}$ the number of descriptions of file f cached at receiver u.
- **Transmission Phase:** After the caching phase, the network is repeatedly used in a time slotted fashion with time slot duration Δ, given by the video segment duration. Each receiver requests one video segment per time slot. Based on the receiver requests, the stored contents at the receiver caches, and the channel conditions, the sender decides at what quality level to send the requested files (i.e., how many descriptions to send to each receiver), encodes the chosen video segments into a codeword, and sends it over the broadcast channel to the receivers, such that each receiver can decode its requested segment (at the scheduled quality level) within Δ channel uses. We denote by d_u the scheduled quality level for receiver u.

[1]As will be shown later, compared to scalable video coding [15], multiple description coding offers significant advantages that are especially relevant for the use of caching-aided coded multicasting.

[2]Because of the time-scale separation between caching and transmission phases, the caching phase is sometimes referred to as the placement or pre-fetching phase.

III. Problem Formulation

As in previous studies for the broadcast caching network, the goal is to characterize the rate-memory region defined as the closure of the set of all achievable rate-memory tuples. While a number of studies have characterized this fundamental tradeoff under error-free channel conditions [4]–[11], only a few recent works have provided first steps towards the characterization of the rate-memory region under a degraded broadcast channel [21], [22]. These studies are however limited to scenarios with only two receivers and unrealistic constraints such as requiring the worst channel receiver to have larger storage capacity. In the following, we introduce an information-theoretic formulation for the general wireless video delivery over a stochastically degraded broadcast channel problem described in Section II.

A. Information-Theoretic Formulation

As stated earlier, we represent the video segments by binary vectors $W_f \in \mathbb{F}_2^F$ of entropy F. At the beginning of time, a realization of the library $\{W_f\}$[3] is revealed to the sender. A $(\Delta, \{\epsilon_u\})$-delivery scheme consists of:

1) Cache Encoder: The sender, given the knowledge of the demand distribution $\mathbf{Q}$ and the cache sizes $\{M_u\}$, fills the caches of the U receivers through a set of U encoding functions $\{Z_u : \mathbb{F}_2^{mF} \to \mathbb{F}_2^{M_u F}\}$, such that $Z_u(\{W_f\})$ denotes the codeword stored in the cache of receiver u.

2) Joint Source-Channel Multicast Encoder: The sender, given the knowledge of the cache configuration $\{Z_u\}$, the channel conditions $\{\epsilon_u\}$, the network time slot duration Δ, and the receiver requests $\mathbf{f}$, schedules the quality level d_u for each requested video segment through a multicast encoder, defined by a variable-to-fixed encoding function $\mathbf{X} : \mathbb{F}_2^{mF} \times \mathcal{F}^U \to \mathbb{F}_2^{\Delta}$ (where $\mathbb{F}_2^{\Delta}$ denotes the set of binary sequences of finite length Δ),[4] such that the transmitted codeword is given by

$$\mathbf{X} \stackrel{\Delta}{=} \mathbf{X}(\{Z_u\}, \{\epsilon_u\}, \mathbf{f}), \tag{4}$$

where $\mathbf{f} \stackrel{\Delta}{=} [f_1, f_2, \ldots, f_U]$, with $f_u \in \mathcal{F}$, denotes the realization of the receiver random request vector $\mathsf{f} = [\mathsf{f}_1, \mathsf{f}_2, \ldots, \mathsf{f}_U]$.

Remark 1: We remark that the classical separation source channel coding over compound channel (SSC-CC), while optimal for equal channel conditions, it is known to be suboptimal in general.

[3]For ease of exposition, in the following, unless specified, we denote by $\{A_i\}$ the full set of elements $\{A_i : i \in I\}$.

[4]The symbol $\mathbb{F}_2^{\Delta}$ is used to indicate that the codeword length is fixed and dictated by the time slot duration Δ.

Remark 2: Note that the variable-to-fixed nature of the multicast encoder is due to the fact that, while the length of the transmitted codeword $\mathbf{X}$ is fixed to the network time slot duration Δ, the amount of information bits transmitted by the encoder is variable and given by $\sum_u d_u B$.

3) Multicast Decoders: Each receiver $u \in \mathcal{U}$, after observing its channel output $\mathbf{Y}_u$, decodes the requested file $W_u \in \mathcal{F}$ as $\widehat{W}_u = \lambda_u(\mathbf{Y}_u, Z_u, \mathbf{f})$, where $\lambda_u : \mathcal{Y}^\Delta \times \mathbb{F}_2^{M_u F} \times \mathcal{F}^U \to \mathbb{F}_2^F$ denotes the decoding function of receiver u (with $\mathcal{Y}^\Delta$ denoting the set of the received sequences).

The worst-case (over the file library) error probability of a $(\Delta, \{\epsilon_u\})$-delivery scheme over a stochastically degraded broadcast channel with channel degradations $\{\epsilon_u\}$ is given by

$$P_e^{(F)}(\mathbf{X}, \{Z_u\}, \{\lambda_u\}, \{\epsilon_u\}) = \sup_{\{W_f\}} \mathbb{P}\left(\bigcup_{u \in \mathcal{U}} \left\{ \widehat{W}_u \neq W_u \right\} \right). \quad (5)$$

Definition 1: A sequence of $(\Delta, \{\epsilon_u\})$-delivery schemes is called *admissible* if

$$\lim_{F \to \infty} P_e^{(F)}(\mathbf{X}, \{Z_u\}, \{\lambda_u\}, \{\epsilon_u\}) = 0.$$

$\Diamond$

B. Average Performance Measures

We define the average *per-receiver delivery rate* of a $(\Delta, \{\epsilon_u\})$-delivery scheme as the average number of bits per channel use provided to receiver u via the combined use of the its own cache and the multicast codeword[5]:

$$R_u^{(F)} = \inf_{\{W_f\}} \frac{B}{\Delta} \left(\mathbb{E}[d_u(\mathsf{f})] + \mathbb{E}[\mu_{u,\mathsf{f}_u}] \right), \quad (6)$$

where $d_u(\mathsf{f})$ and μ_{u,f_u}[6] are the number of descriptions delivered to receiver u via the multicast codeword and via the receiver's cache, respectively, and the expectations are with respect to the random request vector f. Note that $d_u(\mathsf{f}) + \mu_{u,\mathsf{f}_u} \leq D$.

In addition, we can define the average *network delivery rate* of a $(\Delta, \{\epsilon_u\})$-delivery scheme as

$$R^{(F)} = \inf_{\{W_f\}} \frac{B}{\Delta} \sum_{u=1}^{U} \left(\mathbb{E}[d_u(\mathsf{f})] + \mathbb{E}[\mu_{u,\mathsf{f}_u}] \right). \quad (7)$$

Similarly, we define the average *per-receiver distortion* $\delta_u^{(F)}$ and the average *network distortion* $\delta^{(F)}$ of a $(\Delta, \{\epsilon_u\})$-delivery scheme as

$$\delta_u^{(F)} = \sup_{\{W_f\}} \left(1 - \frac{E[d_u(\mathsf{f})] + \mathbb{E}[\mu_{u,\mathsf{f}_u}]}{D} \right), \quad (8)$$

$$\delta^{(F)} = \sup_{\{W_f\}} \left(1 - \frac{1}{U} \sum_{u=1}^{U} \left(\frac{E[d_u(\mathsf{f})] + \mathbb{E}[\mu_{u,\mathsf{f}_u}]}{D} \right) \right). \quad (9)$$

[5]Note that (6) indicates the worst-case (over the library) average (over the demands) *per-receiver delivery rate*.

[6]Recall that f_u denotes the random variable that models the request of receiver u.

Definition 2: A set of average *per-receiver distortions* $(\delta_1, \ldots, \delta_U)$ is achievable if there exists a sequence of admissible $(\Delta, \{\epsilon_u\})$-delivery schemes with average *per-receiver distortions* $(\delta_1^{(F)}, \ldots, \delta_U^{(F)})$ such that

$$\limsup_{F \to \infty} \delta_u^{(F)} \leq \delta_u, \quad \forall u \in \mathcal{U}. \quad (10)$$

$\Diamond$

In the following, we focus on a particular class of admissible $(\Delta, \{\epsilon_u\})$-delivery schemes, based on a specific choice of **Cache Encoder** and joint source-channel **Multicast Encoder**. Specifically, we consider a cache encoder based on random fractional caching [7] and a multicast encoder consisting of a channel-aware index coding scheme that builds on a novel graph coloring algorithm based on *maximal generalized independent sets*. We refer to our solution as Random Popularity Caching and Channel-Aware Chromatic Index Coding (RAP-CA-CIC). RAP-CA-CIC is designed to assure that *i)* all the receivers are able to decode the requested information from the received multicast codeword, and *ii)* no receiver gets affected by receivers with worse channel conditions.

IV. Cache Encoder

The cache encoder exploits the fact that a video segment is multiple description coded into D descriptions, each of length $B = F/D$ bits. In the following, such descriptions are referred to as packets and denoted by $\{W_{f,\ell} : \ell = 1, \ldots, D\}$. The caching phase works as follows. Each receiver, instructed by the sender, randomly selects and stores in its cache a collection of $p_{f,u} M_u D$ distinct packets of file $f \in \mathcal{F}$, where $\mathbf{p}_u = (p_{1,u}, \ldots, p_{m,u})$ is a vector with components $0 \leq p_{f,u} \leq 1/M_u, \forall f$, such that $\sum_{f=1}^m p_{f,u} = 1$, referred to as the caching distribution of receiver u. Hence, the arbitrary element $p_{f,u}$ of $\mathbf{p}_u$ represents the fraction of the memory M_u allocated to file f. The resulting codeword $Z_u(\{W_f\})$ stored in the cache of receiver u is given by

$$Z_u = \Big(W_{1,\ell_{1,1}^u}, \ldots, W_{1,\ell_{1,p_{1,u}M_u D}^u}, W_{2,\ell_{2,1}^u}, \ldots, W_{2,\ell_{1,p_{2,u}M_u D}^u}, \ldots, W_{m,\ell_{m,1}^u}, \ldots, W_{m,\ell_{m,p_{m,u}M_u D}^u} \Big), \quad (11)$$

where $\ell_{f,i}^u$ is the index of the i-th packet of file f cached by receiver u. The tuples of indices $(\ell_{f,1}^u, \ldots, \ell_{f,p_{f,u}M_u D}^u)$ are chosen independently across for each receiver $u \in \mathcal{U}$ and file $f \in \mathcal{F}$, with uniform probability over all $\binom{D}{p_{f,u}M_u D}$ distinct subsets of size $p_{f,u}M_u D$ in the set of D packets of file f. We refer to the random collection of cached packet indices across all receivers as the cache configuration, denoted by $\mathsf{M} = \{Z_u\}$. A given realization of M is denoted by $\mathbf{M}$. Moreover, we denote by $\mathbf{M}_{u,f}$ the vector of indices of the packets of file f cached by receiver u.

The aforementioned caching policy is referred to as *RAndom fractional Popularity-based (RAP) caching*, which is completely characterized by the caching distribution $\mathbf{P} = \{\mathbf{p}_u\}$. RAP is synthesized in Algorithm 1.

We remark that a key property of RAP is that by choosing the identity of the packets to be cached uniformly at random, it increases the number of distinct packets cached across the network. The fact that receivers cache different packets of the

Algorithm 1 RAndom Popularity-Based (RAP) Caching

1: **for all** $f \in \mathcal{F}$ **do**
2: Each receiver $u \in \mathcal{U}$ caches $p_{f,u} M_u D$ distinct packets of file f chosen uniformly at random.
3: **end for**
4: **return** $\mathbf{M} = [\mathbf{M}_{u,f}], u \in \{1, \ldots, U\}, f \in \{1, \ldots, m\}$.

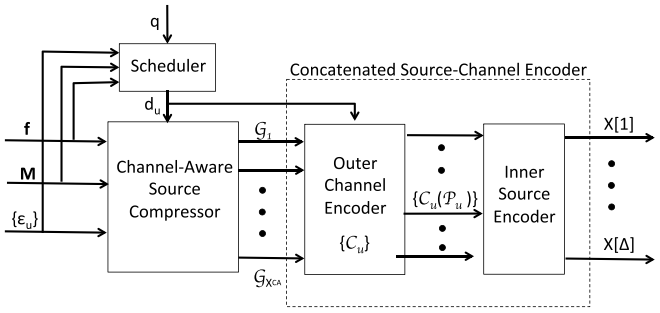

Fig. 2. Joint source-channel multicast encoder.

same file is essential to enable coded multicast opportunities during the transmission phase [7]. This is one of the reasons why multiple description coding is much more suitable than scalable video coding, since randomly cached packets (descriptions) can always be used for decoding higher quality video versions. With scalable video coding, randomly cached descriptions may be wasted if not all previous descriptions are delivered during the transmission phase [23]. While this can be avoided by only caching descriptions up to the maximum number that can be delivered to a given receiver, the resulting reduced amount of overall cached information can lead to reduced coded multicast opportunities. In addition, any deviation due to imperfect knowledge of demand and channel conditions can again lead to wasted cached information, reducing system robustness.

V. Multicast Encoder

The goal of the joint source-channel multicast encoder is to create a multicast codeword that allows each receiver to decode its requested video segment at a rate that is equal to the maximum rate achievable if the remaining $U-1$ receivers had its same channel degradation. The proposed multicast encoder, depicted in Fig. 2, is composed of three main building blocks:

A. Scheduler

Recall that, for a given realization of the packet-level cache configuration $\mathbf{M}$ and the channel rates $\{\eta_u\}$, the joint source-channel multicast encoder is a variable-to-fixed encoder that, at each realization of the request vector $\mathbf{f}$, encodes the scheduled descriptions for each receiver $\{d_u\}$ into a multicast codeword $\mathbf{X}$ of fixed length Δ. The scheduler in Fig. 2 computes the number of descriptions scheduled for receiver u as

$$d_u(\mathbf{f}) = \frac{\Delta \eta_u}{B\,\psi(\mathbf{f}, \mathbf{M})}, \tag{12}$$

where $\psi(\mathbf{f}, \mathbf{M})$ is a function of the packet-level cache realization $\mathbf{M}$ and of the request vector realization $\mathbf{f}$, whose expression is given by Eq. (32) in Appendix.

As will be shown in Appendix, Eq. (12) guarantees that, with a multicast codeword of length Δ, receiver u obtains d_u descriptions (each of size B) at a rate $\eta_u/\psi(\mathbf{f}, \mathbf{M})$, which is the maximum (within a constant factor) rate achievable when the remaining $U-1$ receivers have the same channel degradation η_u [7].

Note from (12) that the number of descriptions depends on $\psi(\mathbf{f}, \mathbf{M})$ and consequently on the cache and demand realizations. This dependence can be specially critical for the concatenated source-channel encoder, possibly requiring channel codebook updates at each request round (see Section V-C). In order to eliminate this overhead, we impose that receiver u obtains d_u descriptions at a rate $\eta_u/\psi(\mathbf{f}, \mathbf{M})$, but set the codeword length given by $d_u B\,\psi(\mathbf{f}, \mathbf{M})/\eta_u$ to be, *in average*, equal to the network time slot duration Δ. In this case, the number of scheduled descriptions for receiver u is given by

$$d_u = \frac{\Delta \eta_u}{B\mathbb{E}[\psi(\mathsf{f}, \mathsf{M})]}, \tag{13}$$

where $\mathbb{E}[\psi(\mathsf{f}, \mathsf{M})]$ is the expectation of $\psi(\mathsf{f}, \mathsf{M})$ taken over the random request vector f and random cache configuration M, whose expression is given by Eq. (21) in Appendix.

Remark 3: Note that, although not explicitly stated in Eqs. (12) and (13), the number of scheduled descriptions for receiver u must be bounded by $D(1 - M_{u,f_u})$.[7] In addition, the ratios $\frac{\Delta \eta_u}{B\psi(\mathbf{f},\mathbf{M})}$ and $\frac{\Delta \eta_u}{B\mathbb{E}[\psi(\mathsf{f},\mathsf{M})]}$ may not be integer and, in practice, would need to be rounded down.

B. Channel-Aware Source Compressor

The goal of the channel-aware source compressor is to cluster the set of packets (descriptions) scheduled for each receiver $\{d_u\}$ into a smaller set of equivalent classes. A key concept driving this process is what we refer to as *generalized independent set* (GIS). As shall be clear from its formal definition in Section VI, the concept of GIS generalizes the classical notion of independent set in the graph coloring literature. The proposed compressor clusters the entire set of scheduled packets (descriptions) into the minimum number of GISs satisfying the following conditions:

- Any two packets in a GIS scheduled for different receivers can be transmitted in the same time-frequency slot without affecting decodability.
- The set of packets in a GIS scheduled for receiver u, denoted by $\mathcal{P}_u$, satisfies

$$\frac{|\mathcal{P}_u|}{\eta_u} = \frac{|\mathcal{P}_i|}{\eta_i}, \quad \forall u, i \in \{1, \ldots, U\}. \tag{14}$$

  Note that (14) makes sure that each receiver is scheduled a number of packets (descriptions) proportional to its channel rate.

As described in detail in Section VI-A, this minimization corresponds to a NP-hard optimization problem related to finding the minimum number of GISs that cover a properly constructed *conflict graph*. We refer to the minimum number of GISs needed to cover the conflict graph as *channel-aware*

[7] Recall that f_u denotes the realization of the file requested by receiver u.

chromatic-number, χ_{CA}, and to the associated transmission scheme as *Channel-Aware Chromatic-number Index Coding (CA-CIC)* (see Section VI-A). Given the exponential complexity of CA-CIC, we then provide in Section VI-B a practical polynomial-time approximation of CA-CIC, referred to as *Channel-Aware Hierarchical greedy Coloring (CA-HgC)*.

C. Concatenated Source-Channel Encoder

The concatenated source-channel encoder generates the multicast codeword $\mathbf{X}$ in which the scheduled descriptions $\{d_u\}$ are encoded. It consists of an outer channel encoder and an inner source encoder. The outer channel encoder generates channel codewords of length n, while the inner source encoder generates the final multicast codeword $\mathbf{X}$ of length Δ, by concatenating linear combinations of n-length channel codewords.

1) Outer Channel Encoder: As illustrated in Fig. 2, the outer channel encoder takes as input the GISs generated by the channel-aware source compressor and, for each GIS and receiver u, encodes the descriptions associated with the set $\mathcal{P}_u$ of entropy $|\mathcal{P}_u|B$ bits, into a codeword $\mathfrak{C}_u(\mathcal{P}_u)$ of length n, via channel codebook $\mathfrak{C}_u$, generated according to the following definition:

Definition 3: An $(2^{n\eta_u}, n)$ code for the u-th binary channel consists of the following:

- An index set $\{1, 2, \ldots, 2^{n\eta_u}\}$;
- An encoding function

$$\mathfrak{C}_u : \{1, 2, \ldots, 2^{n\eta_u}\} \rightarrow \{0, 1\}^n \tag{15}$$

  yielding the codebook $\{\mathfrak{C}_u(1), \ldots \mathfrak{C}_u(2^{n\eta_u})\}$;
- A decoding function

$$g_u : \mathcal{Y}^n \rightarrow \{1, 2, \ldots, 2^{n\eta_u}\}; \tag{16}$$

$\Diamond$

Remark 4: Note that if $\frac{|\mathcal{P}_u|}{\eta_u}B$ is not a multiple of n, then zero-padding is applied to the $|\mathcal{P}_u|B$ bits.

The sender notifies the computed codebooks to each receiver at network setup or anytime channel conditions change. Hence, each receiver is aware, not only of its own codebook, but also of the codebooks of the other receivers.

In line with Section V-A, and as shown in Appendix, in order to guarantee that each receiver obtains d_u descriptions at a rate $\frac{\eta_u}{\psi(\mathbf{f},\mathbf{M})}$, the channel codeword length is set to $n = \frac{\Delta}{\psi(\mathbf{f},\mathbf{M})}$ (see Eq. (12)). The fact that n depends on the demand realization implies that the channel codebook may need to be updated and notified to each receiver at each request round, leading to significant overhead. In order to eliminate this overhead, we set $n = \frac{\Delta}{\mathbb{E}[\psi(\mathsf{f},\mathsf{M})]}$, which, as noted earlier, is equivalent to impose the time slot duration to be equal to the video segment duration *in average*. Note that, although not explicitly stated, the channel codeword length n is upper bounded by $\frac{DB(1-M_{u,f_u})}{\eta_u}$.

2) Inner Source Encoder: Generates the final multicast codeword $\mathbf{X}$ by XORing the channel codewords $\{\mathfrak{C}_u(\mathcal{P}_u)\}$ belonging to the same GIS, and concatenating the resulting codewords of length n.

Recall that the number of GISs produced by the channel-aware source compressor is given by χ_{CA}. Hence, $\mathbf{X}$ is obtained by concatenating χ_{CA} codewords of length n, resulting in a multicast codeword of *average* length Δ, as described in Section VI.

VI. Source Compression Algorithms

In this section, we describe in detail the proposed algorithms for the channel-aware compressor. These algorithms build on generalizations of existing caching-aided coded multicast schemes to the case of noisy broadcast channels. Specifically, Section VI-A describes CA-CIC as the channel aware extension of the chromatic index coding scheme [6], [7], [22], and Section VI-B describes CA-HgC as the channel-aware extension of the polynomial-time hierarchical greedy coloring algorithm [9], [11].

A. Channel-Aware Chromatic Index Coding (CA-CIC)

We recall that finding a coded multicast scheme for the broadcast caching network is equivalent to finding an index code with side information given by the cache realization $\mathbf{M}$ [22]. A well-known index code is given by the chromatic number of the *conflict graph*, constructed according to the demand and cache realizations. Note that, given the cache realization $\mathbf{M}$, a file-level demand realization (given by the request vector $\mathbf{f}$) can be translated into a packet-level request vector containing the missing packets at each receiver. A request for file f_u by receiver u is hence equivalent to requesting $D - |\mathbf{M}_{u,f}|$ packets corresponding to all missing packets of the highest quality level of video segment f_u. However, recall that based on the channel degradations, the sender schedules a subset of the missing packets $d_u \in \{1, \ldots, D(1 - M_{u,f})\}$, as described in Section V-A. We denote by $\mathbf{W}$ the scheduled packet-level configuration and by $\mathbf{W}_{u,f}$ the set of packets of file f scheduled for receiver u. We can then define the corresponding index coding conflict graph $\mathcal{H}_{\mathbf{M},\mathbf{W}} = (\mathcal{V}, \mathcal{E})$ as follows:

- Each vertex $v \in \mathcal{V}$ represents a scheduled packet, uniquely identified by the pair $\{\rho(v), \mu(v)\}$, where $\rho(v)$ indicates the packet identity associated to vertex v and $\mu(v)$ represents the receiver for whom it is scheduled. In total, we have $|\mathcal{V}| = \sum_{u\in\mathcal{U}} d_u$ vertices.
- For any pair of vertices v_1, v_2, we say that vertex v_1 interferes with vertex v_2 if the packet associated to the vertex v_1, $\rho(v_1)$, is not in the cache of the receiver associated to vertex v_2, $\mu(v_2)$, and $\rho(v_1)$ and $\rho(v_2)$ do not represent the same packet. Then, there is an edge between v_1 and v_2 in $\mathcal{E}$ if v_1 interferes with v_2 or v_2 interferes with v_1.

We note that in $\mathcal{H}_{\mathbf{M},\mathbf{W}}$ the set of vertices scheduled for the same receiver, i.e., the set of vertices $v \in \mathcal{V}$ such that $\mu(v) = u$, is fully-connected. Based on this consideration, we refer to $\mathcal{H}_{\mathbf{M},\mathbf{W}}$ as a U-clustered graph.

We now introduce the concept of Generalized Independent Set (GIS) of a U-clustered graph:

Definition 4: We define a $(s_1, \ldots, s_U)$-GIS of a U-clustered graph $\mathcal{H}_{\mathbf{M},\mathbf{W}}$ as a set of U fully connected sub-graphs $\{\mathcal{P}_1, \ldots \mathcal{P}_U\}$ such that for all $u = 1, \ldots, U$:

- For all $v \in \mathcal{P}_u$, $\mu(v) = u$ (i.e., all the packets in $\mathcal{P}_u$ are scheduled for receiver u)
- $|\mathcal{P}_u| = s_u \geq 0$ (i.e., the number of packets in $\mathcal{P}_u$ is equal to s_u)
- For all $i \neq u$, $\mathcal{P}_u$ and $\mathcal{P}_i$ are mutually disconnected (i.e., no edges exist between any two subgraphs) ◊

Note that when $s_u \leq 1, \forall u \in \mathcal{U}$, Def. 4 becomes the classical definition of independent set.

Based on the notion of GIS, we introduce the definition of channel-aware valid coloring and channel-aware chromatic number of the conflict graph:

Definition 5 (Channel-Aware Valid Vertex-Coloring): A $(\eta_1, \ldots, \eta_U)$ channel-aware valid vertex-coloring is obtained by covering the conflict graph $\mathcal{H}_{\mathbf{M},\mathbf{W}}$ with $(s_1, \ldots, s_U)$-GISs that further satisfy $\frac{s_u}{s_i} = \frac{\eta_u}{\eta_i}, \forall u, i \in \{1, \ldots U\}$, and assigning the same color to all the vertices in the same GIS. ◊

Definition 6 (Channel-Aware Chromatic Number): The $(\eta_1, \ldots, \eta_U)$ channel-aware chromatic number of a graph $\mathcal{H}$ is defined as

$$\chi_{\mathrm{CA}}(\mathcal{H}) = \min_{\{\mathcal{C}\}} |\mathcal{C}|, \tag{17}$$

where $\{\mathcal{C}\}$ denotes the set of all $(\eta_1, \ldots, \eta_U)$ channel-aware valid vertex-colorings of $\mathcal{H}$, and $|\mathcal{C}|$ is the total number of colors in $\mathcal{H}$ for the given $(\eta_1, \ldots, \eta_U)$ channel-aware valid vertex-coloring $\mathcal{C}$. ◊

Theorem 1: Given a conflict graph $\mathcal{H}_{\mathbf{M},\mathbf{W}}$ constructed according to packet-level cache realization $\mathbf{M}$, demand realization $\mathbf{f}$, and scheduled random packet-level configuration $\mathbf{W}$, a tight upper-bound for the channel-aware chromatic number $\chi_{CA}(\mathcal{H}_{\mathbf{M},\mathbf{W}})$, when $D, \Delta \to \infty$, is given by $\psi(\mathbf{f}, \mathbf{M})$, i.e.,

$$\chi_{CA}(\mathcal{H}_{\mathbf{M},\mathbf{W}}) = \psi(\mathbf{f}, \mathbf{M}) + o(1/D). \tag{18}$$

□

Proof: See Appendix. ■

As described in Section V-C, the GISs associated to the chromatic number $\chi_{\mathrm{CA}}(\mathcal{H})$ are then used by the concatenated source-channel encoder to generate the final multicast codeword $\mathbf{X}$.

In the following, we provide an example that illustrates the proposed multicast encoder.

Example 1: Consider a network with $U = 3$ receivers, denoted by $\mathcal{U} = \{1, 2, 3\}$, and $m = 3$ files, denoted by $\mathcal{F} = \{W_a, W_b, W_c\}$. The channel rates are $\eta_1 = \frac{1}{2}$, $\eta_2 = \frac{1}{4}, \eta_3 = \frac{1}{4}$, and the time-slot duration is $\Delta = 8$ channel uses. We assume that demand and caching distributions are such that $\mathbb{E}[\psi(\mathsf{f}, \mathsf{M})] = 2$. Each file is multiple description coded into D descriptions, e.g., $W_a = \{W_{a,1}, W_{a,2}, \ldots, W_{a,D}\}$, each of length $B = F/D = 1$ bit. According to Eq. (13), the sender schedules 2 descriptions for receiver 1, i.e., $d_1 = 2$, and one description for receivers 2 and 3, i.e., $d_2 = d_3 = 1$. We assume the caching realization is given by: $\mathbf{M}_{1,W_a} = \{W_{a,1}, W_{a,2}\}$, $\mathbf{M}_{1,W_c} = \{W_{c,1}\}$; $\mathbf{M}_{2,W_b} = \{W_{b,1}, W_{b,2}\}$, $\mathbf{M}_{2,W_c} = \{W_{c,1}\}$; $\mathbf{M}_{3,W_a} = \{W_{a,1}\}$, $\mathbf{M}_{3,W_b} = \{W_{b,1}, W_{b,3}\}$. Suppose receiver 1 requests W_b, receiver 2 requests W_a, and receiver 3 requests W_c such that $\mathbf{W}_{1,W_b} = \{W_{b,1}, W_{b,2}\}$, $\mathbf{W}_{2,W_a} = \{W_{a,1}\}$ and $\mathbf{W}_{3,W_c} = \{W_{c,1}\}$. The corresponding conflict graph $\mathcal{H}_{\mathbf{M},\mathbf{W}}$ is shown in Fig. 3, along with the U-clusters $\{\mathcal{V}_u\}_{u=1}^3$. Each vertex v in $\mathcal{H}_{\mathbf{M},\mathbf{W}}$ is uniquely identified by the pair $\{\rho(v), \mu(v)\}$ with $\rho(v)$ indicating the packet identity and $\mu(v)$ the requesting receiver.

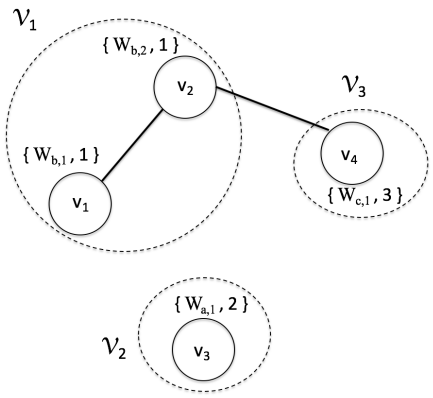

Fig. 3. An example of U-clustered graph $\mathcal{H}_{\mathbf{M},\mathbf{W}}$.

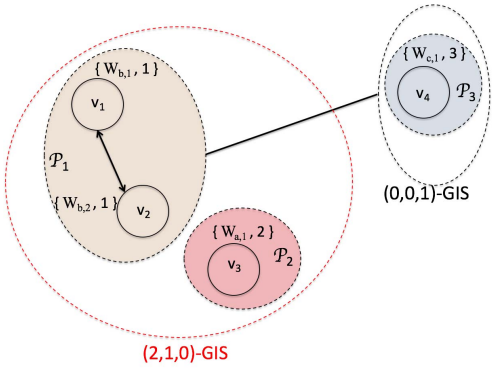

Fig. 4. An example of (s_1, s_2, s_3)-GISs of the 3-clustered graph $\mathcal{H}_{\mathbf{M},\mathbf{W}}$ shown in Fig. 3.

In Figure 4, we show two (s_1, s_2, s_3)-GISs covering the 3-clustered graph $\mathcal{H}_{\mathbf{M},\mathbf{W}}$. The first GIS is composed of two nonempty fully connected sub-graphs: $\mathcal{P}_1 = \{v_1, v_2\}$ with $s_1 = |\mathcal{P}_1| = 2$, and $\mathcal{P}_2 = \{v_3\}$ with $s_2 = |\mathcal{P}_2| = 1$. The second GIS is composed of one non-empty fully connected subgraph: $\mathcal{P}_3 = \{v_4\}$, with $s_3 = |\mathcal{P}_3| = 1$.

The channel-aware vertex coloring is depicted in Fig. 4, with channel-aware chromatic number $\chi_{CA}(\mathcal{H}_{\mathbf{M},\mathbf{W}})$ equal to two colors, one for each GIS (red dotted circle and black dotted circle). The multicast codeword $\mathbf{X}$ of length $\Delta = 8$ is obtained concatenating the codewords $\mathfrak{C}_1(\mathcal{P}_1) \oplus \mathfrak{C}_2(\mathcal{P}_2)$ and $\mathfrak{C}_3(\mathcal{P}_3)$, each of length $n = 4$.

It is important to note that computing the chromatic number of a graph is a well known NP-Hard problem. In the next subsection, we introduce a polynomial-time approximation of CA-CIC, referred to as *Channel-Aware Hierarchical greedy Coloring (CA-HgC)*.

B. Channel-Aware Hierarchical Greedy Coloring (CA-HgC)

We now present Channel-Aware Hierarchical greedy Coloring (CA-HgC), a novel coded multicast algorithm that fully accounts for the broadcast channel impairments, while exhibiting polynomial-time complexity.

Algorithm 2 CA-HgC$_2$

$\mathcal{C} = \emptyset$
$\mathbf{X} = \emptyset$
for $i = U : 1$ **do**
  for $v \in H_i : |\mathcal{K}_v| = \min_{v' \in H_i}\{|\mathcal{K}_{v'}|\}$ **do**
    $[\mathcal{G}, \mathbf{\Omega}] =$`GISfunction`$(H_i, v, i)$
    if $\mathcal{G} \neq \emptyset$ **then**
      $\forall u \in \mathbf{\Omega}$ code the vertices in $\{v' \in \mathcal{G} : \mu(v') = u\}$ with the $\left(\frac{\Delta}{\mathbb{E}[\psi(\mathsf{f},\mathsf{M})]}\right)$–length codeword $\mathfrak{c}_u = \mathfrak{C}_u(\{v' \in \mathcal{G} : \mu(v') = u\})$ in the codebook $\mathfrak{C}_u$
      $\mathbf{X} = [\mathbf{X} \sum_{u \in \mathbf{\Omega}} \otimes \mathfrak{c}_u]$
      color $(\sum_{u \in \mathbf{\Omega}} \otimes \mathfrak{c}_u)$ by $\alpha \notin \mathcal{C}$
      $H_i = H_i \setminus \mathcal{G}$
    else
      $H_i = H_i \setminus \{v\}$; $H_{i-1} = H_{i-1} \cup \{v\}$
    end if
  end for
end for
return $|\mathcal{C}|$, $\mathbf{X}$

The CA-HgC algorithm works by computing two valid colorings of the conflict graph $\mathcal{H}_{\mathbf{M},\mathbf{W}}$, referred to as CA-HgC$_1$ and CA-HgC$_2$. CA-HgC then compares the corresponding number of colors achieved by the two solutions and selects the coloring with minimum number of colors. We note that CA-HgC$_1$ coincides with the conventional naive (uncoded) multicast scheme. In fact, CA-HgC$_1$ computes the minimum coloring of $\mathcal{H}_{\mathbf{M},\mathbf{W}}$ subject to the constraint that only the vertices representing the same packet are allowed to have the same color. In this case, the total number of colors is equal to the number of distinct requested packets, and the coloring can be found in $O(|\mathcal{V}|^2)$. On the other hand, CA-HgC$_2$ is described by Algorithm 2, in which the subroutine `GISfunction`$(\cdot,\cdot,\cdot)$ is defined by Algorithm 3. It can be shown that the complexity of CA-HgC$_2$ is given by $O(U|\mathcal{V}|^2)$, i.e., it is polynomial in $|\mathcal{V}|$.

In the following, we first guide the reader through Algorithm 2 and then we provide an illustrative example.[8]

Let $\mathcal{K}_v \triangleq \{u \in \mathcal{U} : \rho(v) \in \mathbf{W}_u \cup \mathbf{M}_u\}$ denote the set of receivers that request and/or cache packet $\rho(v)$. We start by initializing the i-th vertex hierarchy in of $\mathcal{H}_{\mathbf{M},\mathbf{W}}$ to the set of vertices for whom the number of receivers requesting and/or caching its packet identity is equal to i, i.e., $\mathcal{H}_i \triangleq \{v : |\mathcal{K}_v| = i\}$. CA-HgC$_2$ proceeds in decreasing order of hierarchy starting from the U-th hierarchy.

For each vertex v in the i-th hierarchy in increasing order of cardinality $|\mathcal{K}_v|$, we call the subroutine `GISfunction`$(\mathcal{H}_i, v, i)$. If the subroutine returns a non-empty set $\mathcal{G}$, then we color the vertices in $\mathcal{G}$ with the same color (lines 6-10). Otherwise, we move the uncolored vertex v to the next hierarchy, i.e., $\mathcal{H}_{i-1}$ (lines 11-12). This procedure is iteratively applied for any hierarchy, until all the vertices in the conflict graph $\mathcal{H}_{\mathbf{M},\mathbf{W}}$ are colored. The procedure returns the number of colors $|\mathcal{C}|$ as well as the set of codewords $\mathbf{X}$.

[8]With a slight abuse of notation, we denote by $\mathfrak{c}_u = \mathfrak{C}_u(\{v' \in \mathcal{G} : \mu(v') = u\})$ the codeword obtained by coding the Bs_u source bits associated to the packets $\{\rho(v') : \mu(v') = u\}$.

Algorithm 3 `GISfunction`(H_i, v, i)

1: $\mathcal{G} = \{v\}$; $\mathbf{\Omega} = \{\mu(v)\}$; $\tilde{H}_i = H_i$
2: **for** $v' \in \tilde{H}_i \setminus \mathcal{G} : |\mathcal{K}_{v'}| = \min_{v'' \in \tilde{H}_i \setminus \mathcal{G}}\{|\mathcal{K}_{v''}|\}$ **do**
3: **if** no edge between v' and $\mathcal{G}$ **then**
4: $\mathcal{G} = \mathcal{G} \cup \{v'\}$; $\mathbf{\Omega} = \mathbf{\Omega} \cup \{\mu(v')\}$
5: **else**
6: $\tilde{H}_i = \tilde{H}_i \setminus \{v'\}$
7: **end if**
8: **end for**
9: **if** $|\mathcal{G}| \geq i$ **then**
10: **for** $v' \in \tilde{H}_i \setminus \mathcal{G} : |\mathcal{K}_{v'}| = \min_{v'' \in \tilde{H}_i \setminus \mathcal{G}}\{|\mathcal{K}_{v''}|\} \wedge \mu(v') \in \mathbf{\Omega}$ **do**
11: $\mathcal{G}_{\mu(v')} = \{v" \in \mathcal{G} : \mu(v") = \mu(v')\}$
12: **if** $|\mathcal{G}_{\mu(v')}| < d_{\mu(v')}$ and no edge between v' and $\mathcal{G} \setminus \mathcal{G}_{\mu(v')}$ **then**
13: $\mathcal{G} = \mathcal{G} \cup \{v'\}$
14: **else**
15: $\tilde{H}_i = \tilde{H}_i \setminus \{v'\}$
16: **end if**
17: **end for**
18: **return** $\mathcal{G}$, $\mathbf{\Omega}$
19: **else**
20: **return** $\mathcal{G} = \emptyset$, $\mathbf{\Omega} = \emptyset$
21: **end if**

Regarding the subroutine `GISfunction`$(\mathcal{H}_i, v, i)$ shown in Algorithm 3, we initially set $\mathcal{G} = \{v\}$. Then, for each vertex $v' \in \mathcal{H}_i$ in increasing order of cardinality $|\mathcal{K}_{v'}|$, we move v' into $\mathcal{G}$ if v' is not connected (via the conflict graph) to any node currently in $\mathcal{G}$ (lines 2-8). Note that in the first iteration the lowest cardinality in $\mathcal{H}_i$ is exactly equal to i. By construction, each vertex in the conflict graph has an associated receiver, hence we denote by $\mathbf{\Omega}$ the set of receivers associated to the vertices in $\mathcal{G}$. If $\mathcal{G} < i$, i.e., if we were not able to select at least i vertices, then we return two empty sets (lines 19-20). Otherwise, we proceed by trying to select, for each receiver $\mu(v') \in \mathbf{\Omega}$, $d_{\mu(v')} - 1$ additional lowest-cardinality vertices in $\mathcal{H}_i$ having no links with the vertices in $\mathcal{G}$ associated to receivers different from $\mu(v')$ (lines 10-17). If we succeed (or if the considered hierarchy is 1, meaning that we have no further hierarchies to explore), then we return the set of selected vertices $\mathcal{G}$ as well as the set of associated receivers $\mathbf{\Omega}$ (line 18).

Example 2: Consider the same conflict graph $\mathcal{H}_{\mathbf{M},\mathbf{W}}$ shown in Fig. 3 and let us apply Algorithm 2. We start by constructing $\mathcal{K}_v$ by inspection of the conflict graph: $\mathcal{K}_{v_1} = \{1,2,3\}$, $\mathcal{K}_{v_2} = \{1,2\}$, $\mathcal{K}_{v_3} = \{1,2,3\}$, and $\mathcal{K}_{v_4} = \{1,2,3\}$. Hence, $\mathcal{H}_U = H_3 = \{v_1, v_3, v_4\}$, $\mathcal{H}_2 = \{v_2\}$, and $\mathcal{H}_1 = \emptyset$. Starting from the highest hierarchy, in line 5 of Algorithm 2 we call the subroutine GISfunction with parameters $\mathcal{H}_3$, v_1 and 3. By running iteratively the proposed algorithm, the GISs shown in Fig. 4 are obtained.

VII. Multicast Decoder

In this section, we analyze the decodability of the proposed achievable scheme.

From the observation of its channel output $\mathbf{Y}_u$, representing its noisy version of the transmitted codeword $\mathbf{X}$, receiver u decodes the d_u descriptions of its requested video segment $W_u \in \mathcal{F}$ scheduled and transmitted by the sender as $\widehat{W}_u = \lambda_u(\mathbf{Y}_u, Z_u, \mathbf{f})$, via its own decoding function λ_u, which consists of two stages:

- First, receiver u is informed (e.g., via packet header information) of the sub-codewords in the concatenated multicast codeword $\mathbf{X}$ that contain any of its scheduled descriptions. For each of the identified sub-codewords, receiver u obtains the noisy version of its channel codeword $\mathfrak{C}_u(j)$ with $j \in \{1, \ldots, 2^{n\eta_u}\}$ by performing the inverse XOR function. To this end, receiver u is informed of the packets and their intended receivers that are present in the XORed sub-codeword. Receiver u can then construct the channel codewords associated to the other receivers from its cached information and the corresponding codebooks (recall that every receiver is informed of all the channel codebooks) and recover its own codeword $\mathfrak{C}_u(j)$ via inverse XORing.
- Then, the recovered noisy codeword $\mathfrak{C}_u(j)$ is sent to the channel decoder of receiver u, which reconstructs the bits associated to the set $\mathcal{P}_u$ according to the channel rate η_u.

Hence, according to Def. 1, in the limit $D \to \infty$, the proposed sequence of $(\Delta, \{\epsilon_u\})$-delivery schemes is *admissible.*

A. Achievable Delivery Rates

It is immediate to verify that the $(\Delta, \{\epsilon_u\})$-delivery schemes RAP-CA-CIC and RAP-CA-HgC generate a sequence of admissible schemes as per Def. 1. In the following, we provide an explicit expression for the average per-receiver and network delivery rates, formally defined in Eqs. (6)-(7), achieved by the proposed $(\Delta, \{\epsilon_u\})$-delivery schemes when $F, D, \Delta \to \infty$ with the ratios $B = F/D$ and $\gamma = \Delta/F$ kept constant. For ease of exposition, we assume $p_{f,u} = p_f$, $q_{f,u} = q_f$, and $M_u = M, \forall u \in \mathcal{U}$.[9]

Theorem 2: The average per-receiver and network delivery rates achieved by the $(\Delta, \{\epsilon_u\})$-delivery schemes RAP-CA-CIC and RAP-HgCAC, as $F, D, \Delta \to \infty$, satisfy:

$$\begin{aligned} &R_u^{\mathrm{CA-CIC}}(U, m, M, \{\epsilon_u\}) \\ &\geq R_u^{\mathrm{CA-HgC}}(U, m, M, \{\epsilon_u\}) \\ &\geq \min\left\{\frac{\eta_u}{\mathbb{E}[\psi(\mathsf{f}, \mathsf{M})]}, \frac{(1 - \mathbb{E}[M_{u,\mathsf{f}_u}])}{\gamma}\right\} + \frac{\mathbb{E}[M_{u,\mathsf{f}_u}]}{\gamma}, \end{aligned} \tag{19}$$

$$\begin{aligned} &R^{\mathrm{CA-CIC}}(U, m, M, \{\epsilon_u\}) \\ &\geq R^{\mathrm{CA-HgC}}(U, m, M, \{\epsilon_u\}) \\ &\geq \sum_{u=1}^{U}\left(\min\left\{\frac{\eta_u}{\mathbb{E}[\psi(\mathsf{f}, \mathsf{M})]}, \frac{(1 - \mathbb{E}[M_{u,\mathsf{f}_u}])}{\gamma}\right\} + \frac{\mathbb{E}[M_{u,\mathsf{f}_u}]}{\gamma}\right), \end{aligned} \tag{20}$$

where

$$\mathbb{E}[\psi(\mathsf{f}, \mathsf{M})] = \min\{\phi(\mathbf{p}, \mathbf{Q}), \bar{m}\}, \tag{21}$$

[9]The generalization to the case of different $\{p_{f,u}\}$, $\{q_{f,u}\}$ and $\{M_u\}$ across receivers is immediately obtained by replacing Eqs. (22)-(23) with Eqs. (2)-(3) in [10].

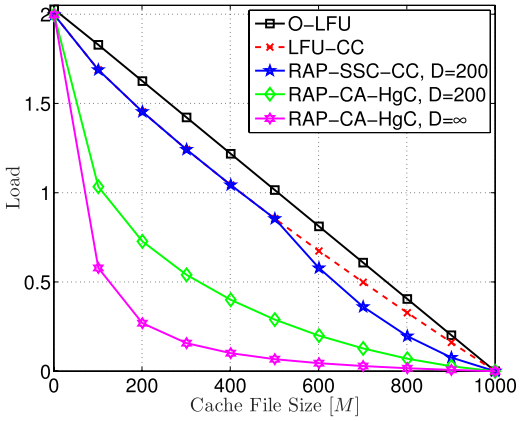

Fig. 5. Average load in a broadcast caching network with $m = 1000$, $U = 30$, $\alpha = 0.2$.

with

$$\bar{m} = \sum_{f=1}^{m}\left(1 - \left(1 - q_f\right)^U\right),$$

$$\phi(\mathbf{p}, \mathbf{Q}) = \sum_{f=1}^{m}\sum_{\ell=1}^{U}\binom{U}{\ell}\rho_{f,\ell}(1 - p_f M)^{U-\ell+1}(p_f M)^{\ell-1}, \tag{22}$$

$$\rho_{f,\ell} \stackrel{\Delta}{=} \mathbb{P}(f = arg\max_{j \in \Upsilon}(p_j M)^{\ell-1}(1 - p_j M)^{n-\ell+1}), \tag{23}$$

and Υ denoting a random set of ℓ elements selected in an i.i.d. manner from $\mathcal{F}$ (with replacement). □

Proof: See Appendix. ■

Remark 5: Observe from Eq. (19) that, in contrast with the classical SSC-CC solution, our proposed channel-aware caching-aided coded multicast solutions guarantee that no receiver gets affected by receivers with worse channel conditions.

VIII. Validation of the Theoretical Results

The goal of this section is provide numerical validation of the theoretical results given in Section VII-A. Specifically, we analyze the performance of RAP-CA-HgC for finite file packetization (i.e., finite number of video descriptions) compared with: *i)* LFU caching with Compound Channel transmission (i.e., naive multicasting at the rate of the worse channel receiver), referred to as LFU-CC; *ii)* LFU caching with unicast transmission, referred to as orthogonal LFU (O-LFU); *iii)* RAP caching with separate source-channel coding over compound channel with HgC as source encoder, referred to as RAP-SSC-CC; and *iv)* the benchmark upper bound (RAP-CA-HgC) when $D = \infty$ (Theorem 2).

We consider a network with $m = 1000$ files and $U = 30$ receivers with channel rates uniformly distributed among three values usually used in LTE standards: $\{\eta_1 = \frac{1}{2}, \eta_2 = \frac{3}{4}, \eta_3 = \frac{1}{4}\}$. We assume that receivers request files according to a common Zipf demand distribution with $\alpha = \{0.2, 0.4\}$, all caches have size M files, and the maximum number of descriptions is $D = 200$.

Figs. 5 and 6 show numerical results in terms of *network load*, defined as the inverse of the *network transmission rate*,

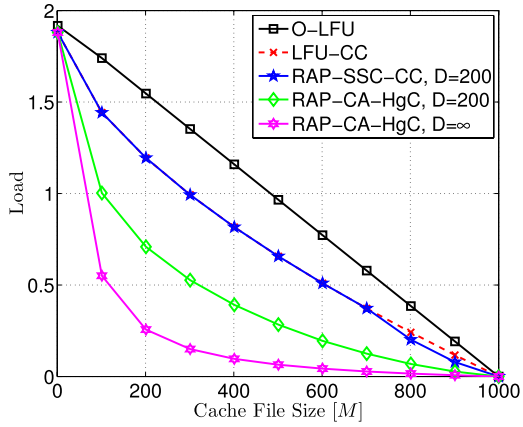

Fig. 6. Average load in a broadcast caching network with $m = 1000$, $U = 30$, $\alpha = 0.4$.

and given by $\frac{\mathbb{E}[\psi(\mathsf{f},\mathsf{M})]}{\sum_{u=1}^{U}\mathbb{E}[\eta_u(\mathsf{f})]}$, as shown in Theorem 2. This metric is specially illustrative of the the amount of bandwidth resources the wireless operator needs to provide in order to meet the receiver demands.

In Fig. 5, we assume a Zipf parameter $\alpha = 0.2$. Observe first the performance of LFU. As expected, the load reduces approximately linearly with the cache size M. Note that while a channel-unaware caching-aided coded multicast scheme such as RAP-SSC-CC is able to achieve smaller network loads than LFU for all values of M, the reduction is limited by the adverse effect of the heterogeneous channel conditions on the coded multicast transmission. In fact the performance of RAP-SSC-CC is essentially the same as that of LFU-CC, clearly showing the vanishing benefit of coded multicasting under heterogeneous channel conditions. Observe now the performance of the proposed RAP-CA-HgC with $D = \infty$. The reduction of network load with cache size resembles the remarkable multiplicative caching gains of the caching-aided coded multicast schemes under error-free broadcast channel [6]–[8]. This clearly shows the effectiveness of RAP-CA-HgC in allowing receivers to decode their requested video segments without being affected by receivers with worse channel conditions. Note that RAP-CA-HgC achieves network load reductions that are $7\times$ larger than LFU for $M = 200$ (20% of the library size). Importantly, the more practical RAP-CA-HgC with $D = 200$ is able to preserve the multiplicative rate-memory tradeoff, with a notorious $4\times$ load reduction with respect to LFU for $M = 200$.

Note that very similar trends are observed in Fig. 6, where the Zipf parameter is set to $\alpha = 0.4$, confirming the superiority of RAP-CA-HgC in exploiting the remarkable benefits of caching-aided coded multicast video delivery schemes, while avoiding critical penalizations from the presence of receivers with worse channel conditions.

IX. Conclusions

In this paper, we design and analyze a novel wireless video delivery scheme that specifically addresses the pressing need to accommodate next-generation video-based services over increasingly crowded and bandwidth-limited wireless access networks. We consider a heterogeneous wireless edge caching architecture where the cache-enabled receivers (e.g., helpers) are connected to the sender by lossy links. We provide an information theoretic formulation for the channel aware caching-aided coded multicast problem and design two achievable schemes, RAP-CA-CIC and RAP-CA-HgC, which result from the careful implementation of joint source-channel coding into the caching-aided coded multicast problem. Our solutions preserve the cache-enabled multiplicative throughput gains of the uniform channel scenario, completely avoiding throughput penalizations from the presence of receivers experiencing worse propagation conditions.

Appendix
Proof of Theorems 1 and 2

In the following, we analytically quantify the performance of the RAP-CA-HgC and, by extension, of RAP-CA-CIC.

For mathematical tractability, we relax RAP-CA-HgC by removing the conditions in line 9 of Algorithm 3. This forces the construction of a GIS to happen within a given hierarchy, without taking into account the uncolored vertices from higher hierarchies.[10] This implies that any GIS, $\mathcal{G}$, generated by Algorithm 2 is composed of vertices belonging to the same hierarchy, i.e., $\forall v, v' \in \mathcal{G}, \mathcal{K}_v = \mathcal{K}_{v'}$. This allows us to associate any GIS, $\mathcal{G}$, generated by Algorithm 2 and belonging to the ℓ-th hierarchy with a given subset of ℓ receivers, $\mathcal{U}^\ell$, such that $\mathcal{K}_v = \mathcal{U}^\ell$ for any $v \in \mathcal{G}$.

Let $\mathcal{I}(\mathcal{U}^\ell)$ be the $(s_1, \ldots, s_U)$-GIS associated with $\mathcal{U}^\ell$, i.e., the GIS for which $s_u = 0$ if $u \notin \mathcal{U}^\ell$, with $\ell = 1, \ldots, U$. Denoting by $|\mathcal{I}(\mathcal{U}^\ell)|$ the number of coded bits associated with $\mathcal{I}(\mathcal{U}^\ell)$, we have

$$|\mathcal{I}(\mathcal{U}^\ell)| = \max_{f \in \mathbf{f}(\mathcal{U}^\ell)} \left\{ \left\lceil \frac{B}{\eta_{\mu(v)}} \sum_{v:\rho(v)\ni f} 1\{\mathcal{K}_v = \mathcal{U}^\ell\} \right\rceil \right\}, \quad (24)$$

where $\mathbf{f}(\mathcal{U}^\ell)$ represents the set of files requested by $\mathcal{U}^\ell$ and the indicator $1\{\mathcal{K}_v = \mathcal{U}^\ell\}$ denotes the event that packet $\rho(v)$ requested by receiver $\mu(v) \in \mathcal{U}^\ell$ is cached at all receivers $\mathcal{U}^\ell \setminus \{\mu(v)\}$ and not cached at any other receiver. Note that $1\{\mathcal{K}_v = \mathcal{U}^\ell\}$ follows a Bernoulli distribution with parameter

$$\lambda(f, \ell) = (p_f M)^{\ell-1}(1 - p_f M)^{U-\ell+1}. \quad (25)$$

Denoting by $d_{\mu(v)}$ the scheduled descriptions for receiver $\mu(v)$, and by exploiting the Bernoulli distribution of $1\{\mathcal{K}_v = \mathcal{U}^\ell\}$, with high probability, we have

$$\sum_{v:\rho(v)\ni f_{\mu(v)}} 1\{\mathcal{K}_v = \mathcal{U}^\ell\} = \lambda(f, \ell) d_{\mu(v)} + \delta(D), \quad (26)$$

with $\delta(D) \to 0$ as $D \to \infty$.

Substituting (26) in (24), we obtain

$$|\mathcal{I}(\mathcal{U}^\ell)| = \max_{f \in \mathbf{f}(\mathcal{U}^\ell)} \left\{ \left\lceil \frac{B}{\eta_{\mu(v)}} \left(\lambda(f, \ell) d_{\mu(v)} + \delta(D)\right) \right\rceil \right\}. \quad (27)$$

[10] This in general returns a less efficient covering of the graph, i.e., a larger number of disjoint GISs covering the graph. However, as proved in [7] when $D \to \infty$ this provides a tight upper bound.

By assumption (see Eq. (12)), we set $d_{\mu(v)}$, which represents the cardinality of the set $\{v : \rho(v) \ni f_{\mu(v)}\}$, such that

$$\frac{B}{\eta_{\mu(v)}} d_{\mu(v)} = \min\left\{\frac{\Delta}{\psi(\mathbf{f},\mathbf{M})}, \frac{BD(1-p_{f_u}M)}{\eta_{\mu(v)}}\right\}. \quad (28)$$

If $\frac{\Delta}{\psi(\mathbf{f},\mathbf{M})} < \frac{BD(1-p_{f_u}M)}{\eta_{\mu(v)}}$, then, from (28), it also follows that if the channel codeword length is given by $n = \frac{\Delta}{\psi(\mathbf{f},\mathbf{M})}$, then only one channel codeword per receiver is associated to each GIS. Hence, from the scheme described in Section V-C, the number of codewords that the inner source encoder concatenates is equal to the number of GISs, and the total number of coded bits is

$$\Delta = n\chi_{\mathrm{CA}}(\mathcal{H}_{\mathbf{M},\mathbf{W}}). \quad (29)$$

By substituting (28) in (27), we have

$$|\mathcal{I}(\mathcal{U}^\ell)| = \max_{f\in\mathbf{f}(\mathcal{U}^\ell)}\left\{\left\lceil \frac{\Delta}{\psi(\mathbf{f},\mathbf{M})}(\lambda(f,\ell)+o(1/D))\right\rceil\right\}.$$

As $D\to\infty$, with high probability,

$$|\mathcal{I}(\mathcal{U}^\ell)| = \max_{f_u\in\mathbf{f}(\mathcal{U}^\ell)} \frac{\Delta}{\psi(\mathbf{f},\mathbf{M})}\lambda(f,\ell), \quad (30)$$

from which the total number of coded bits is given by

$$\sum_{\ell=1}^{U}\sum_{\mathcal{U}^\ell\subset\mathcal{U}}\left|\mathcal{I}(\mathcal{U}^\ell)\right| = \frac{\Delta}{\psi(\mathbf{f},\mathbf{M})}\sum_{\ell=1}^{U}\binom{U}{\ell}\max_{f_u\in\mathbf{f}(\mathcal{U}^\ell)}\lambda(f,\ell). \quad (31)$$

From (31), in order to satisfy the time-slot duration constraint Δ, we need

$$\psi(\mathbf{f},\mathbf{M}) = \sum_{\ell=1}^{U}\binom{U}{\ell}\max_{f_u\in\mathbf{f}(\mathcal{U}^\ell)}\lambda(f,\ell). \quad (32)$$

Furthemore, from (29) and (31), it follows that $\psi(\mathbf{f},\mathbf{M}) = \chi_{\mathrm{CA}}(\mathcal{H}_{\mathbf{M},\mathbf{W}})$ from which Theorem 1 follows. By averaging (32) over the demand distribution, we obtain that $\psi(\mathrm{f},\mathrm{M})$ concentrates its probability mass in $\mathbb{E}[\psi(\mathbf{f},\mathbf{M})]$ with

$$\mathbb{E}[\psi(\mathbf{f},\mathbf{M})] = \sum_{f=1}^{m}\sum_{\ell=1}^{U}\binom{U}{\ell}\rho_{f,\ell}\lambda(f,\ell), \quad (33)$$

where $\rho_{f,\ell}$ is given in (23), from which the first term of the minimum in (21) follows. The second term follows directly from [7], [9].

If $\frac{\Delta}{\psi(\mathbf{f},\mathbf{M})} \geq \frac{BD(1-p_{f_u}M)}{\eta_{\mu(v)}}$, then $\frac{Bd_{\mu(v)}}{\Delta} = \frac{BD(1-p_{f_u}M)}{\Delta} = \frac{(1-p_{f_u}M)}{\gamma}$, from which the third term in (21) follows, concluding the proof of Theorem 2.

REFERENCES

[1] Cisco Global Cloud Index. (Nov. 2014). *Forecast and Methodology, 2013–2018*. [Online]. Available: http://www.cisco.com/c/en/us/solutions/collateral/service-provider/global-cloud-index-gci/Cloud_Index_White_Paper.html

[2] Cisco Visual Networking Index. (Feb. 2015). *Globe Mobile Data Traffic Forecast Update, 2014–2019*. [Online]. Available: http://www.cisco.com/c/en/us/solutions/collateral/service-provider/visual-networking-index-vni/mobile-white-paper-c11-520862.html

[3] N. Golrezaei, A. F. Molisch, A. G. Dimakis, and G. Caire, "Femtocaching and device-to-device collaboration: A new architecture for wireless video distribution," *IEEE Commun. Mag.*, vol. 51, no. 4, pp. 142–149, Apr. 2013.

[4] M. A. Maddah-Ali and U. Niesen. (2012). "Fundamental limits of caching." [Online]. Available: http://arxiv.org/abs/1209.5807

[5] M. Maddah-Ali and U. Niesen, "Decentralized coded caching attains order-optimal memory-rate tradeoff," *IEEE/ACM Trans. Netw.*, vol. 23, no. 4, pp. 1029–1040, Aug. 2015.

[6] M. Ji, A. M. Tulino, J. Llorca, and G. Caire, "On the average performance of caching and coded multicasting with random demands," in *Proc. 11th Int. Symp. Wireless Commun. Syst. (ISWCS)*, Aug. 2014, pp. 922–926.

[7] M. Ji, A. M. Tulino, J. Llorca, and G. Caire. (2015). "Order-optimal rate of caching and coded multicasting with random demands." [Online]. Available: http://arxiv.org/abs/1502.03124

[8] M. Ji, A. M. Tulino, J. Llorca, and G. Caire, "Caching and coded multicasting: Multiple groupcast index coding," in *Proc. IEEE Global Conf. Signal Inf. Process. (GlobalSIP)*, Dec. 2014, pp. 881–885.

[9] M. Ji, K. Shanmugam, G. Vettigli, J. Llorca, A. Tulino, and G. Caire, "An efficient multiple-groupcast coded multicasting scheme for finite fractional caching," in *Proc. IEEE Int. Conf. Commun. (ICC)*, Jun. 2015, pp. 3801–3806.

[10] G. Vettigli, M. Ji, A. M. Tulino, J. Llorca, and P. Festa, "An efficient coded multicasting scheme preserving the multiplicative caching gain," in *Proc. IEEE Conf. Comput. Commun. Workshops (INFOCOM WKSHPS)*, Apr./May 2015, pp. 251–256.

[11] K. Shanmugam, M. Ji, A. M. Tulino, J. Llorca, and A. G. Dimkakis, "Finite length analysis of caching-aided coded multicasting," in *Proc. Annu. Allerton Conf. Commun., Control, Comput.*, Oct. 2014, pp. 914–920.

[12] P. A. Chou, H. J. Wang, and V. N. Padmanabhan, "Layered multiple description coding," in *Proc. Packet Video Workshop*, Apr. 2003, p. 4.

[13] S. Pudlewski, N. Cen, Z. Guan, and T. Melodia, "Video transmission over lossy wireless networks: A cross-layer perspective," *IEEE J. Sel. Topics Signal Process.*, vol. 9, no. 1, pp. 6–21, Feb. 2015.

[14] A. El Gamal, "The capacity of a class of broadcast channels," *IEEE Trans. Inf. Theory*, vol. 25, no. 2, pp. 166–169, Mar. 1979.

[15] H. Schwarz, D. Marpe, and T. Wiegand, "Overview of the scalable video coding extension of the H.264/AVC standard," *IEEE Trans. Circuits Syst. Video Technol.*, vol. 17, no. 9, pp. 1103–1120, Sep. 2007.

[16] S. Kokalj-Filipović, E. Soljanin, and Y. Gao, "Cliff effect suppression through multiple-descriptions with split personality," in *Proc. IEEE Int. Symp. Inform. Theory (ISIT)*, Jul./Aug. 2011, pp. 948–952.

[17] H. Ketmaneechairat, P. Oothongsap, and P. Mingkhwan, "Buffer size estimation for different start video broadcasting," in *Proc. Int. Conf. Elect. Eng./Electron. Comput. Telecommun. Inf. Technol. (ECTI-CON)*, May 2010, pp. 924–928.

[18] J. Korner and K. Marton, "General broadcast channels with degraded message sets," *IEEE Trans. Inf. Theory*, vol. 23, no. 1, pp. 60–64, Jan. 1977.

[19] R. G. Gallager, "Capacity and coding for degraded broadcast channels," *Probl. Peredachi Inf.*, vol. 10, no. 3, pp. 3–14, Jul./Sep. 1974.

[20] A. S. Mansour, R. F. Schaefer, and H. Boche. (2015). "On the capacity of broadcast channels with degraded message sets and message cognition under different secrecy constraints." [Online]. Available: http://arxiv.org/abs/1501.04490

[21] B. Asadi, L. Ong, and S. J. Johnson. (2015). "A unified scheme for two-receiver broadcast channels with receiver message side information." [Online]. Available: http://arxiv.org/abs/1504.00082

[22] R. Timo and M. A. Wigger, "Joint cache-channel coding over erasure broadcast channels," in *Proc. Int. Symp. Wireless Commun. Syst. (ISWCS)*, Aug. 2015, pp. 201–205.

[23] L. P. Hassanzadeh, E. Erkip, J. Llorca, and A. Tulino, "Distortion-memory tradeoffs in cache-aided wireless video delivery," in *Proc. Allerton Conf. Commun., Control, Comput.*, Sep./Oct. 2015, pp. 1150–1157.

Angela Sara Cacciapuoti (M'10–SM'16) received the D.Eng. (*summa cum laude*) degree in telecommunications engineering and the Ph.D. (Hons.) degree in electronic and telecommunications engineering from the University of Naples Federico II in 2005 and 2009, respectively. She was a Visiting Researcher with the Broadband Wireless Networking Laboratory, Georgia Institute of Technology, Atlanta, GA, USA, from 2010 to 2011, and the NaNoNetworking Center, Catalunya, Universitat Politecnica de Catalunya, Barcelona, Spain, in 2011. She is currently an Assistant Professor with the DIETI Department, University of Naples Federico II. Since 2014, she has been an Area Editor of *Computer Networks* (Elsevier). Her current research interests are in Internet of Things, nanonetworks, 5G mobile networks, and neuronal models.

Marcello Caleffi (M'12–SM'16) received the D.Eng. (*summa cum laude*) degree in computer science engineering from the University of Lecce, Lecce, Italy, in 2005, and the Ph.D. degree in electronic and telecommunications engineering from the University of Naples Federico II, Naples, Italy, in 2009. He was a Visiting Researcher with the Broadband Wireless Networking Laboratory, Georgia Institute of Technology, Atlanta, GA, USA, from 2010 to 2011, and the NaNoNetworking Center, Catalunya, Universitat Politecnica de Catalunya, Barcelona, Spain, in 2011. He is an Assistant Professor with the DIETI Department, University of Naples Federico II, where he teaches telematics and mobile communication systems classes and supervised and graduated more than 20 students among the B.S. and M.S. students. Since 2014, he has been an Area Editor of *Elsevier Ad Hoc Networks*. His research interests are cognitive radio networks, biological networks, and nanonetworks. He has co-authored over 40 journal (IEEE TRANSACTIONS ON NETWORKING/*ACM Transactions on Networking*, the IEEE TRANSACTIONS ON WIRELESS COMMUNICATIONS, the IEEE TRANSACTIONS ON COMMUNICATIONS, the IEEE TRANSACTIONS ON VEHICULAR TECHNOLOGY, and the IEEE INTERNET OF THINGS JOURNAL) and conference (the IEEE Globecom, the IEEE ICC, the IEEE SECON, and ACM NANOCOM) publications.

Mingyue Ji (S'09–M'15) received the bachelor's degree in communication engineering from the Beijing University of Posts and Telecommunications, China, the M.S. degree in electrical engineering from the Royal Institute of Technology, Sweden, and the Ph.D. degree from the Ming Hsieh Department of Electrical Engineering, University of Southern California (USC), under the supervision of Prof. G. Caire. He was a Research Engineer and finished his master's thesis with the Access Technologies and Signal Processing Group, Ericsson, Stockholm, Sweden. He is a Staff II, System Design Scientist with Broadcom Ltd.

His main interests are in the fields of information theory, coding theory, concentration of measure, stochastic network optimization, and statistics with the applications of caching networks, wireless communications, distributed storage and computing, and (statistical) signal processing. He received the Best Paper Award at the IEEE ICC 2015 conference, the Best Student Paper Award at the IEEE European Wireless 2010 Conference, and the USC Annenberg Fellowship from 2010 to 2014.

Jaime Llorca (S'05–M'09) received the B.S. degree in electrical engineering from the Universidad Politecnica de Catalunya, Barcelona, Spain, in 2001, and the M.S. and Ph.D. degrees in electrical and computer engineering from the University of Maryland, College Park, MD, USA, in 2003 and 2008, respectively. He held a post-doctoral position with the Center for Networking of Infrastructure Sensors, College Park, MD, USA, from 2008 to 2010. He has been a Communication Networks Research Scientist with Bell Laboratories, Holmdel, NJ, USA, since 2010. He has authored over 50 peer-reviewed articles and more than 10 patents. His research interests include energy efficient networks, distributed cloud networking, content distribution, resource allocation, network information theory, and network optimization. He received the 2007 International Conference on Sensors, Sensor Networks, and Information Processing (ISSNIP) Best Paper Award, the 2016 International Conference on Communications (ICC) Best Paper Award, and the 2015 Jimmy H. C. Lin Award for Innovation.

Antonia Maria Tulino (F'13) received the Ph.D. degree in electrical engineering from the Seconda Università degli Studi di Napoli, Italy, in 1999. She held research positions with Princeton University, the Center for Wireless Communications, Oulu, Finland, and the Università degli Studi del Sannio, Benevento, Italy. Since 2002, she is Associate Professor at the Università degli Studi di Napoli Federico II. In 2009 she has joined Bell Labs, Nokia. Her research interests lay in the area of communication systems approached with the complementary tools provided by signal processing, information theory, and random matrix theory. Since 2011, she has been a member of the Editorial Board of the IEEE TRANSACTIONS ON INFORMATION THEORY. She has received several paper awards and, among others, the 2009 Stephen O. Rice Prize in the field of communications theory for the best paper in the IEEE TRANSACTIONS ON COMMUNICATION in 2008. She has been a Principal Investigator of several research projects sponsored by the European Union and the Italian National Council, and was selected by the National Academy of Engineering for the Frontiers of Engineering program in 2013.